# Observations of Neutral Atoms from the Solar Wind

Michael R. Collier[1], Thomas E. Moore[1], Keith W. Ogilvie[1],
Dennis Chornay[1,2], J.W. Keller[1], S. Boardsen[1,9], James Burch[3], B. El Marji[1,2],
M.-C. Fok[1], S.A. Fuselier[4], A.G. Ghielmetti[4], B.L. Giles[1], D.C. Hamilton[2],
B.L. Peko[5], J.M. Quinn[6], E.C. Roelof[10], T.M. Stephen[5], G.R. Wilson[7] and P. Wurz[8]

1. NASA/Goddard Space Flight Center, Greenbelt, Maryland
2. University of Maryland, College Park
3. Southwest Research Institute, San Antonio, Texas
4. Lockheed Martin Advanced Technology Center, Palo Alto, California
5. University of Denver, Colorado
6. University of New Hampshire, Durham
7. Mission Research Corporation, Nashua, New Hampshire
8. University of Bern, Switzerland
9. Raytheon ITSS Corporation, Lanham, Maryland
10. The Johns Hopkins University/Applied Physics Laboratory, Laurel, Maryland

date: 29 December 2000 – version: 4.4

**Abstract.** We report observations of neutral atoms from the solar wind in the Earth's vicinity with the Low Energy Neutral Atom (LENA) imager on the IMAGE spacecraft. This instrument was designed to be capable of looking at and in the direction of the Sun. Enhancements in the hydrogen count rate in the solar direction are not correlated with either solar ultraviolet emission or suprathermal ions and are deduced to be due to neutral particles from the solar wind. LENA observes these particles from the direction closest to that of the Sun even when the Sun is not directly in LENA's 90° field-of-view. Simulations show these neutrals are the result of solar wind ions charge-exchanging with exospheric neutral hydrogen atoms in the post-shock flow of the solar wind in the magnetosheath. Their energy is inferred to exceed 300 eV, consistent with solar wind energies, based on simulation results and on the observation of oxygen ions, sputtered from the conversion surface in the time-of-flight (TOF) spectra. In addition, the sputtered oxygen abundance tracks the solar wind speed, even when IMAGE is deep inside the magnetosphere. These

results show that low energy neutral atom imaging provides the capability to directly monitor the solar wind flow in the magnetosheath from inside the magnetosphere because there is a continuous and significant flux of neutral atoms originating from the solar wind that permeates the magnetosphere.

## 1. Introduction

The Low Energy Neutral Atom (LENA) imager is one of six science experiments that were launched on the IMAGE observatory on March 25, 2000. This instrument was designed to accomplish remote sensing of the neutral component of space plasmas at energies from a few tens to a few thousands of electron volts [*Moore et al.,* 2000]. Neutral particles in this energy range, which encompasses most of the plasma in the heliosphere, can result when energetic particles charge exchange with the Earth's hydrogen geocorona [*Williams et al.,* 1992] and have not previously been systematically observed. Similar to instruments which image more energetic neutral atoms, LENA has the ability not only to detect the neutral atoms, but also determine their mass, energy and direction (polar and azimuthal angles) [*Hsieh et al.,* 1992a; *Wurz et al.,* 1995]. LENA was designed to observe in the solar direction and responds to neutrals of energies of the order of 1 keV. Consequently, the instrument is capable of observing the fraction of the solar wind flow that is neutral hydrogen, which has been long-recognized as of potentially great importance for understanding solar, interplanetary and magnetospheric physics [*Akasofu,* 1964a,b].

Charge exchange between solar wind protons and neutral atoms can be primarily responsible for the formation of a neutral solar wind, although there is also a neutral component due to recombination of solar wind ions with solar wind elec-

trons [*Gruntman,* 1994]. These charge-exchanging neutrals may be interstellar neutral atoms, they may originate from dust grains [*Holzer,* 1977; *Schwadron et al.,* 2000] or they may be part of the Earth's geocorona. The potential importance of charge exchange with exospheric neutrals may be motivated by the realization that the neutral density at the nominal magnetopause ($\sim 10$ $R_E$) is comparable to the average solar wind density ($\sim 10$ $cm^{-3}$) [*Rairden et al.,* 1986]. Since charge exchange in the geocorona will occur preferentially near the Earth, the neutral solar wind characteristics may be heavily influenced by magnetospheric structures and activity. This can lead to wider angular profiles with signals coming from directions offset from what might be expected from solar wind charge exchange upstream of the Earth's bowshock. These effects will be discussed in more detail in Section 6 entitled "Magnetosheath Charge Exchange Simulations." In addition, if the Earth is in conjunction with Venus, LENA might observe an increased neutral solar wind flux due to charge exchange in the atmosphere of Venus.

The effect of solar wind charge exchange on the exosphere of Venus may be estimated by noting that the fraction of the solar wind density that is neutralized due to an interaction over a characteristic scale length of L is $\sim \sigma$nL where $\sigma$ is the charge exchange cross section and n is the neutral density. Adopting a hydrogen neutral density of about $10^4$ $cm^{-3}$ based on an ionopause height of about 1000 km, a characteristic scale length of about $L = 2$ $R_V = 1.2\text{x}10^9$ cm and a cross section $H^+ + H \rightarrow H + H^+$, $\sigma \sim 10^{-15}$ $cm^{-2}$, we get a neutral solar wind fraction of about $10^{-2}$ at Venus [*Hodges and Tinsley,* 1981; *Bauske et al.,* 1998]. This signal, if observable at 1 AU, will only be seen for a short time during conjunction. However, the outflow of energetic neutral atoms from Venus might be observed, since energetic ions from Venus have been detected at Earth at L1 during conjunction [*Grünwaldt*

*et al.,* 1997].

This paper is organized as follows: Section 1 provides an introduction and overview. Section 2 puts the work into an historical context. Section 3 provides a brief description of the LENA instrument operation. Section 4 describes the general properties of the LENA data with specific emphasis on the omnipresent "Sun pulse" which represents neutral atoms. Data from a specific event from May 24, 2000 when the Sun was in LENA's field-of-view are correlated with solar wind flux. Section 5 discusses an event on June 8, 2000, in which LENA again observed an enhancement in the Sun pulse at the time of an increase in solar wind flux. During the main enhancement on the May 24, 2000 event and most of the June 8, 2000 event, IMAGE was inside the magnetosphere. In the June 8, 2000 event, LENA observed an enhancement even though the Sun was outside of LENA's $\pm 45°$ field-of-view. Section 6 suggests that this unexpected behavior is due to solar wind charge exchange with the geocorona by using simulations. Section 7 provides estimates of the neutral atom flux, compares these to expectations and argues that much of the signal may be due to charge exchange with the geocorona. Section 8 describes the implications of this work on previous proposals by Akasofu [1964a,b], Gruntman [1994], and Hsieh *et al.* [1992b]. Finally, Section 9 is a brief conclusion.

## 2. Historical Context

Historically, the idea that solar wind protons would interact with the Earth's geocorona dates back at least forty years to Dessler *et al.* [1961] who considered this mechanism a potential source of background hydrogen atom flux for observations of proton ring current decay by charge exchange with hydrogen atoms. It is interesting that this mechanism appears to predate that which is currently viewed as

the primary process responsible for creating the neutral solar wind, namely charge exchange with interstellar neutrals. Fahr [1968] suggested that charge exchange between solar wind protons and neutral hydrogen near the Sun would create a neutral solar wind which would penetrate into the thermosphere and produce temperature and density increases. Hundhausen *et al.* [1968] also mention that protons could charge exchange with neutral hydrogen in interplanetary space but did not pursue the discussion because this process would produce no change in the ionization state of the plasma. Holzer [1977] examined the consequences of interplanetary atomic hydrogen on the solar wind and concluded that charge transfer would produce a neutral solar wind to total solar wind flux ratio of about $3\text{x}10^{-5}$ at 1 AU. An outstanding account of the historical development of neutral atom imaging instrumentation can be found in Gruntman [1997].

## 3. LENA Instrument Operation

Figure 1 shows a cross section of the LENA instrument. Neutral atoms (1) enter the instrument through a collimator (2) which rejects charged particles. The collimator operates by placing alternately positive and negative potentials across consecutive horizontal plates. Although designed to handle up to about $\pm 8$ kV, or 16 kV across adjacent plates, LENA has not yet been commanded above half this level or $\pm 4$ kV. In-flight data indicate that at least near apogee under most conditions it is sufficient to have only a couple kilovolts across the collimator plates to eliminate the bulk of the penetrating charged particles.

Neutral particles then hit a tungsten conversion surface (3) at a low angle where a small fraction, of the order of a percent, of the incident neutrals pick up an electron and become negative ions. The conversion surface is held at a high negative

voltage, designed for 20 kV, but run at up to 16.4 kV during calibration and, so far, up to 12 kV in-flight. Following conversion on the tungsten surface, the negative ion "sees" the negative potential of the conversion surface and is accelerated (4) through an extraction lens designed to focus particles spatially in one direction dependent on energy and in the other spatial direction dependent on azimuthal angle (in and out of the paper in Fig. 1). The particles then traverse a tuned hemispherical deflection system (5) and enter the time-of-flight (TOF) unit, which also has a position sensing capability.

In the TOF/position sensing assembly, the spatial information on azimuthal angle and energy produced by the extraction lens is measured using wedge and strip anode position sensing on secondary electrons created when the negative ions traverse a 1.9 $\mu$g/cm$^2$ carbon foil at the front of the unit. Secondary electrons also form the start signal used for a time-of-flight measurement, which determines mass because the energy is fixed by the extraction lens voltage. The particle itself produces the stop signal by traversing the TOF unit and triggering a stop microchannel plate stack.

One feature complicating the LENA data analysis is that neutral atoms hitting the tungsten surface create sputtered particles which have a wide energy distribution and make analysis of the energy data difficult. Fortunately, calibration data show that incident atomic hydrogen begins to sputter statistically significant amounts of oxygen off the tungsten surface somewhere between 300 eV and 1000 eV. This sputtered oxygen is detected by the TOF unit and can be used to broadly determine incident atomic hydrogen energy. This will be discussed in more detail in Section 5 entitled "Observations from the June 8, 2000 Event."

Note that with reference to Fig. 1, the reason why LENA, unlike other neutral

atom imagers, can look directly at the Sun is that for a photon to hit the start or stop microchannel plate stacks, it first must reflect off the conversion surface, then pass the hemispherical deflection system by multiple reflections and finally penetrate the 1.9 $\mu$g/cm$^2$ carbon foil at the front of the time-of-flight unit. After this, a photon must reflect off the wires forming the mirror or some other internal surface in the time-of-flight unit to finally hit the start detector. Consequently, LENA has an extremely low direct sensitivity to photons. However, residual gas in the instrument can be ionized by ultraviolet light, get accelerated by the negative voltage on the conversion surface and produce sputtered particles creating valid events. This mode is clearly pressure dependent, effected by gas inside the instrument. Calibration runs at $\sim 10^{-6}$ Torr with an ultraviolet source suggest that in flight the pressure is too low to produce any significant count rate and, as will be shown, a comparison between in-flight LENA data and SOHO/SEM data corroborates this.

Table 1 lists some of the important LENA instrument characteristics. A complete description of the LENA instrument is given in Moore *et al.* [2000]. LENA data are available to the general public at the same time they are available to the LENA team at http://goewin.gsfc.nasa.gov/LENA/.

## 4. Overview of LENA Sun Pulse Observations

Many clear and consistent features appeared in the LENA data immediately upon reaching science level operations. Figure 2 shows some of these features on May 24, 2000, shortly after LENA reached science level, in the form of a spectrogram which plots the time of day along the x-axis and the LENA spin angle along the y-axis. The color indicates the total event rate, irrespective of the time-of-flight. As mentioned in the previous section, LENA images in two angles, although only

one is plotted in the spectrogram format.

One notable feature is the bright yellow/orange streak which begins near 180° and drifts through all angles. This "Sun pulse" (as it will hereafter be called) appears at the spin angle closest to the solar direction. On this particular day, the Sun was within LENA's ±45° field-of-view and the Sun pulse is actually in the direction of the Sun. Note that when IMAGE moves behind the Earth, the angular range of which is indicated by the white lines, the Sun pulse is occulted. On the June 8, 2000 event, the spin direction about 180° away from the Earth is closest to the Sun and so the Sun pulse appears there during the event, even though the Sun is outside LENA's field-of-view. It was apparent early in the mission that not only did the signal from the Earth respond to solar wind pressure variations, but that the intensity of the Sun pulse did, as well.

Figure 3 shows an example of an increase in the Sun sector LENA count rate resulting from an increase in solar wind flux. The solar wind number flux, measured by WIND about 45 $R_E$ upstream and about 6 $R_E$ off the Sun-Earth line is indicated by the upper, dashed-line trace and the right hand y-axis. The LENA Sun sector hydrogen counts per spin are plotted with the lower solid trace and the left hand y-axis. There are a number of short-lived enhancements in the solar wind flux which are not obviously associated with enhancements in the LENA rate. These are possibly or likely small structures in the solar wind and because WIND and IMAGE are offset from each other perpendicular to the Sun-Earth line by from about 9 $R_E$ to over 11 $R_E$ during the time period covered by Fig. 3, it may not be surprising that LENA does not see them [*Paularena et al.,* 1998]. However, the largest enhancement in solar wind flux, which is observed at about 0200 UT, accompanies a simultaneous enhancement in the LENA Sun sector hydrogen rate.

Ultraviolet data from SOHO show that there was no enhancement at this time so that the increase in the LENA count rate cannot be due to any sensitivity to light.

During this May 24, 2000 event, the collimators, which filter out charged particles, had a potential of about 3.6 kV across the plates, eliminating all ions with energies up to about 20 keV/e while above about 40 keV/e most ions can traverse the collimator and arrive inside the instrument. Evidence from Radio Plasma Imager (RPI) data [*Reinisch et al.,* 2000] indicates that during the main enhancement around 0200 UT IMAGE was inside the magnetosphere [J. Green, private communication], so LENA was not observing ions from the solar wind, and magnetospheric energetic particles would not arrive primarily from the Sun direction, so we conclude that LENA is not responding to charged particles during this event.

In the next section, we will discuss in detail observations similar to the May 24, 2000 event made by LENA on June 8, 2000. The major difference was that this event occurred after May 26, 2000 when the LENA data suggest the component of the neutral solar wind due to charge exchange upstream of the bowshock moved outside of LENA's field-of-view. Nevertheless, LENA still observed a Sun pulse which is due to charge exchange between the broad sheath flow and the Earth's hydrogen geocorona. June 8, 2000 was chosen for detailed analysis to complement other LENA data analysis efforts which focussed on this event.

## 5. Observations from the June 8, 2000 Event

About one month after beginning science operations on May 5, 2000, LENA had an opportunity to observe a coronal mass ejection (CME) and its effect on the terrestrial environment [*Moore et al.*, 2001; *Fuselier et al.*, 2001]. On June 6, 2000, an intense solar flare was observed and was followed by a full-halo CME propagat-

ing toward the Earth. The shock wave driven by this CME was observed by the Advanced Composition Explorer (ACE) and the Solar and Heliospheric Observatory (SOHO) spacecraft at about 0842 UT on June 8, 2000 at the L1 point, 235 $R_E$ upstream from the Earth, and by the WIND spacecraft, 41 $R_E$ upstream, at about 0905 UT [Space Weather News for June 8, 2000, http://www.spaceweather.com; SOHO data available through Dr. F. Ipavich]. At 0911 UT this disturbance passed the Earth where it and its effects were observed by the IMAGE spacecraft. Figure 4 shows a cartoon of the IMAGE geometry along with LENA's field-of-view during this event.

Figure 5 shows a LENA spectrogram of the combined hydrogen and oxygen count rate as a function of time on the day the CME-driven shock passed the Earth, June 8, 2000. Also see the first two panels of Plate 3 of Moore *et al.* [2001] for an image of the sun pulse brightening. The Sun pulse, in time, near 180° is a signal initially thought to represent a response to the EUV photon flux from the Sun. The angular range of the Earth is indicated by the dashed white lines, and the yellow brightening around 0950 UT is the oxygen burst discussed by Fuselier *et al.* [2001]. However, when the sun pulse increased significantly at the arrival of a shock (at 0911 UT) in the solar wind associated with the CME, it was concluded that at least part of this signal must represent neutral atoms in the solar wind (Fuselier *et al.* [2001] discuss the brightening around the Earth direction at 0911 UT and suggest it may be due to high energy (several keV) neutral hydrogen resulting from ion outflow at the arrival of the shock).

As mentioned in Section 3 entitled "LENA Instrument Operation," the LENA UV response is a result of the ionization of particles inside the instrument by photons, as light does not penetrate to the microchannel plates (see Fig. 1). Thus,

the instrument UV response scales with pressure at or near the conversion surface, and the response to UV based on calibration data scaled to the ambient pressures expected on orbit shows that LENA has a negligible UV response there.

As additional evidence that LENA is not responding to UV, Figure 6 shows the EUV data from SOHO [*Judge et al.,* 1998] during June 6-8, 2000. The upper solid line shows the photon flux between 0.1 and 50 nm and the lower dashed curve shows the photon flux between 24 and 34 nm. Note however that this does not include the potentially important hydrogen Lyman-$\alpha$ line at 122 nm. We anticipate, though, that the wavelength ranges shown reflect the behavior of the Lyman-$\alpha$, at least qualitatively. The activity on June 6 associated with the CME is apparent in the data with some subsequent activity on June 7 (which was not associated with a LENA count rate enhancement). During the event on June 8, indicated by the vertical line, there is no enhancement in the EUV flux, indicating that the enhancement seen in the sun pulse by LENA is not due to an increase in solar EUV.

UV radiation can be excluded as the cause of the observed enhancement in the Sun pulse. However, we next consider the possibility that the increase is due to suprathermal ions penetrating the collimator [*Moore et al.,* 2000]. At the time of the June 8, 2000, event a potential of about 8.8 kV was across the collimator (significantly higher than the collimator setting during the May 24, 2000 event) to filter out all ions with energies up to about 50 keV/e, while above about 100 keV/e most ions can traverse the collimator and arrive inside the instrument. The gap between the collimator plates varies from about 20 mm at the front to about 12 mm at the back, so that the electric field varies from 444 to 730 kV/m over a distance of 93 mm. Because ion spectra at these energies in most space plasma environments follow rapidly decreasing power laws [*Collier et al.,* 1993], the primary contributor

to the energetic ion flux entering LENA is likely close to 50 keV/e.

Thus the enhanced sun pulse seen in LENA observations could be due to ions with energies at or above 50 keV/e. If this had been the case, such ions would have been observed by the Electron, Proton, and Alpha Monitor (EPAM) aboard the ACE spacecraft. Figure 7 compares the LENA background-adjusted counts per spin (light trace, left hand y-axis) from the solar direction with the ACE/EPAM ion flux data (heavy trace, right hand y-axis, plotted logarithmically) for this event. The counting rate contained in the LENA data peaks shortly after the shock's passage and slowly decreases for about an hour thereafter. The ACE/EPAM flux data for ions with energies between 47 and 65 keV/e, which includes the 50 keV/e low energy limit for LENA ion admittance, show a step-function type increase by a factor of 25-50 at the time of the shock. If the LENA response were due to these energetic ions, we would expect the time profiles for the observations to be much more similar. This suggests that the enhanced sun pulse observed by LENA is not due to these suprathermal ions.

The conclusion that the sun pulse enhancement is not due to suprathermal ions is also supported by observations by the WIND spacecraft and magnetopause modeling. Figure 8 shows the solar wind ram pressure observed by the WIND spacecraft (with dashed lines on the right hand y-axis). The times when the high latitude magnetopause model of Boardsen *et al.* [2000] predicted that IMAGE was inside the magnetosphere are indicated by the black bars on the top x-axis. Radio Plasma Imager (RPI) data [*Reinisch et al.,* 2000] also suggest that IMAGE exited the magnetosphere during this time period [J. Green, private communication]. The WIND spacecraft at this time was about 41 $R_E$ upstream and about 27 $R_E$ off the Sun-Earth line in the minus $y_{GSE}$ direction. The IMAGE spacecraft, which has

an apogee of about 8 $R_E$, is always within a few $R_E$ in the $y_{GSE}$ direction of the Earth so that the distance between WIND and IMAGE perpendicular to the Sun-Earth line is well within the ~40 $R_E$ scale length inferred by Collier *et al.* [1998] for interplanetary magnetic field correlations, making it likely that WIND was a reliable interplanetary monitor. Although the Boardsen *et al.* model predicts that IMAGE moved across the magnetopause eight times in this three hour period, there are no sudden jumps in the LENA count rate associated with these crossings, as would be expected in ion data at energies around 80 keV [*Paschalidis et al.,* 1994]. Furthermore, when IMAGE is inside the magnetosphere, we would not expect the energetic ions to arrive from a narrow range of directions as the Sun pulse does. In short, the observed enhancement cannot be explained by energetic ions either from the inside of or outside of the magnetosphere.

We conclude LENA observed neutral particles from the solar direction during this event, indicating the Sun pulse was and in general is primarily due to neutral particles. We now address the issue of whether or not the neutral atom energies are consistent with solar wind-like energies of the order of 1-5 keV. Figure 9 shows LENA calibration data taken at the University of Denver neutral beam facility [*Stephen et al.,* 1996]. The upper panel shows a time-of-flight spectrum resulting from incident 30 eV atomic hydrogen. There is a well-defined hydrogen peak at low times-of-flight with no evidence of an oxygen peak. An oxygen peak appears when the energy of the incident neutral hydrogen exceeds a threshold between 300 eV and 1000 eV. Above this threshold, as shown in the lower panel of Fig. 9 for 1000 eV atomic hydrogen, a significant oxygen peak is present, believed to be due to the sputtering of oxygen from oxide or water on the conversion surface.

Figure 10 shows a time-of-flight spectrum taken during the enhancement on

June 8, 2000. The spectrum only includes events coming from the general direction of the Sun. Note the prominent oxygen peak. Since large neutral oxygen fluxes will not be present in the solar wind, this suggests the neutral hydrogen has an energy clearly above 300 eV, at which sputtering can occur. This is consistent with solar wind energies during this time period. In addition to the hydrogen and oxygen peaks, there is a third peak which appears in the in-flight data but was not observed in the calibration data. This may be due to data artifacts because in flight the instrument is running at a higher start microchannel plate bias level. One possibility, because this peak occurs at a lower time-of-flight than the hydrogen peak, is that it results from ringing in the start electronics. If the stop signal is associated with the ringing rather than the original signal, the apparent time-of-flight will be shorter. The higher microchannel plate bias level produces a higher gain which may cause the ringing to be prominent enough to trigger on. Under normal instrument working conditions, a real peak cannot exist at lower times-of-flight than the hydrogen peak because this would imply a mass per charge less than unity.

There is a relatively larger oxygen signal in Fig. 10, the in-flight data, as compared to Fig. 9, the calibration data. Because LENA was only calibrated to 1 keV, we cannot make any quantitative statements about the energies of the neutral hydrogen except that they are greater than 300 eV, based on the appearance of sputtered oxygen at 1 keV, the only atomic hydrogen energy run performed above 300 eV. There are at least two explanations for the larger oxygen signal in the in-flight data as compared to the calibration data: (i) Because of the viewing geometry and the conclusion that LENA is observing charge exchange in the magnetosheath where the suprathermal population is pronounced, LENA may be responding to energies

far greater than 1 keV. During the CME, the solar wind speed was about 750 km/s or roughly 4 keV per nucleon. If the sputtered oxygen yield is a strongly increasing function of energy, this could explain the disparity between the in-flight and calibration hydrogen to oxygen ratio. (ii) The start microchannel plate bias level was lower during calibration (1850 V) than in-flight (1950 V) and there is evidence that the oxygen and hydrogen efficiencies vary differently with microchannel plate bias level [*Oberheide et al.,* 1997; *Barat et al.,* 2000].

The ratio of hydrogen to oxygen in the LENA time-of-flight spectrum may be used to monitor solar wind speed from inside the magnetosphere. The left hand y-axis and solid line in Figure 11 show, as a function of time, the solar wind speed as observed by the Solar Wind Experiment (SWE) on WIND. The right hand y-axis and solid circles indicate the background-adjusted integrated hydrogen to oxygen count ratio in the sun sector from hourly averaged TOF spectra. Prior to the shock passage, the ratio is $0.29 \pm 0.01$ while after the shock passage the ratio is $0.46 \pm 0.05$ indicating that LENA has observed the solar wind speed increase from inside the magnetosphere.

The calibration results suggest the relative amount of oxygen increases with increasing hydrogen atom energy at least up to 1 keV. However, as shown in Figure 11, the relative amount of oxygen appears to go down after the shock. Although it is clear that the ratio does show the transition, there are at least two possible reasons why the hydrogen to oxygen ratio increases, rather than decreases, across the shock: (i) As stated earlier, LENA was only calibrated to 1 keV at which energy the sputtered oxygen was seen (it was not statistically present at 300 eV). Thus, it is not known how the yield of sputtered oxygen versus hydrogen varies with incident atomic hydrogen energy. Fig. 11 shows that there is a composition signature

clearly associated with the solar wind velocity jump, and there is no reason to anticipate any of the observed oxygen comes from the solar wind. If we assume that LENA is, in fact, observing higher atomic hydrogen energies after the shock based on solar wind observations, then this composition change is an instrument effect, likely due to the details of the physics on the tungsten conversion surface. It is known that negative ion sputtering yields at these energies change dramatically with incident beam energy [e.g. *Walton et al.,* 1998; *Vogan et al.,* 2000], so it is not surprising that this ratio would change. However, anion emission yields over this energy range for atomic hydrogen on tungsten to the best of our knowledge have not been measured. (ii) During the June 8, 2000 event, simulations indicate that LENA is monitoring the magnetosheath in which case the data shown in Fig. 11 reflect behavior along the particular line of sight in the magnetosheath LENA is sampling. Thus, it is possible that although the solar wind speed increases across the shock, the integrated line of sight LENA is observing in the magnetosheath may be characterized by lower energies following the shock, depending on how the magnetosheath reconfigures. Although perhaps not a likely possibility, this could, in principle, be addressed by simulations.

## 6. Magnetosheath Charge Exchange Simulations

When the Sun moved out of LENA's field-of-view, the Sun pulse was still visible; one possible explanation is that LENA was observing solar wind charge exchange in the magnetosheath. Because the solar wind in the magnetosheath is deflected, heated, and has pronounced suprathermal tails, all factors that would contribute to observing charge exchange products far off the Sun-Earth line, this explanation seemed plausible. Furthermore, some evidence suggests [e.g. *Bertaux*

*and Blamont,* 1973; *Rairden et al.* 1986] that the neutral hydrogen forms a geotail around the Earth with enhanced densities as one moves more anti-sunward. This would provide additional neutral density with which sheath flow on the flanks could charge-exchange. In addition, a simple calculation, discussed in the next section, showed that the flux would be high enough for LENA to observe.

To check this idea, we have performed simulations of LENA's response on June 8, 2000 to solar wind ions charge exchanging with the Earth's hydrogen geocorona in the magnetosheath. The magnetosheath model is given by a global MHD simulation [*Groth et al.,* 2000]. Figure 12 is an example for 4 keV hydrogen shown in spectrogram format like the LENA data in Fig. 2 and Fig. 5. Note that LENA's response integrates over all energies although the simulations indicate that the major contributors to the LENA response during this event are particles with energies around 4 keV. Note also that this simulation does not include any neutral component in the solar wind that does not result from charge exchange with the Earth's geocorona, i.e., the direct neutral solar wind. Nor does it include any time variation in the magnetosheath. In addition, the simulation does not account for the LENA instrument efficiencies. Finally, the simulation does not invoke suprathermal tails which are pronounced in both the solar wind [*Collier et al.,* 1996] and magnetosheath [*Formisano et al.,* 1973].

The simulation constructs a neutral atom flux image from line of sight (LOS) integrations through the convolution of a spherical geocoronal model [*Rairden et al.,* 1986] and a single fluid MHD simulation of the solar wind and magnetosphere [*Groth et al.,* 2000]. To isolate the solar wind and magnetosheath interaction with the geocorona, the LOS integration runs along rays emanating from the spacecraft position at each point in time, from an inner boundary at 8 $R_E$ to 50 $R_E$, in all

directions except for a 90° cone centered on the negative $x_{SM}$ direction. At each point along the LOS, the directional neutral flux is taken from a drifting Maxwellian distribution with parameters given by the MHD simulation, and convolved with the local geocoronal density and appropriate charge exchange cross section for the given energy. The net result is a nearly all-sky map of the LENA flux on the pixels of the LENA imager.

The results shown in Figure 12 are similar to what LENA observes on June 8, 2000, namely a wide Sun pulse around 180°, the direction closest to the direction of the Sun and suggest that in fact LENA is responding primarily to solar wind charge exchange in the magnetosheath during this event. A simple calculation in the next section shows that solar wind charge exchange with the Earth's geocorona will be comparable to estimates of the neutral solar wind component at 1 AU.

## 7. Neutral Atom Source and Comparison to Expected Fluxes

LENA has observed a neutral particle component in the solar wind. These observations can be used to estimate the neutral flux during the enhancement period, which will be compared to expectations. As shown in Fig. 8, the count rate during the enhancement is about 15 counts per spin. Since each spin sector is observed for about 2.7 seconds, this reduces to a count rate of 5.6 $s^{-1}$. At solar wind energies, LENA's neutral hydrogen detection efficiency was measured to be about $6.4 \times 10^{-5}$. We regard this as being correct to within a factor of two, considering the different conditions in flight and the scatter of the data in the efficiency curves. LENA's entrance aperture has an area of 1 $cm^2$, which yields a flux of about $8.8 \times 10^4$ $cm^{-2}s^{-1}$. At that time, the solar wind flux was $\sim 10^9$ $cm^{-2}s^{-1}$ (12 $cm^{-3}$ density and 800 km/s speed) yielding a flux ratio of neutrals to solar wind protons of about $10^{-4}$.

This value is comparable to the expected neutral solar wind component at 1 AU [*Holzer,* 1977; *Gruntman,* 1994]. However, given the IMAGE orbit on June 8, 2000, and the imager field-of-view, the signal has an apparent origin centered more than 45° from the solar direction and so may originate largely from the magnetosheath interaction with geocoronal hydrogen. As mentioned earlier, a significantly stronger localized signal was observed prior to May 26, 2000 (see Fig. 2), before the solar direction passed beyond the nominal imager field-of-view.

Referring back to Fig. 4, at the time of the June 8, 2000 event, the direct neutral solar wind was on the edge of LENA's nominal field-of-view, so LENA was probably observing solar wind ions charge exchanging in the near-Earth magnetosheath.

To illustrate the potential importance of charge exchange with the Earth's geocorona, we will show a simple estimate of the expected fraction of the flux signal resulting from this effect. The hydrogen atom distribution in the geocorona is a smoothly varying function of the distance from the center of the planet. Using the geocoronal density N(R) as

$$\mathrm{N(R)} = 10 \cdot \left(\frac{11}{\mathrm{R}}\right)^3 \mathrm{cm}^{-3}, \tag{1}$$

where R is the distance from the Earth in Earth radii, we can calculate the neutral atom flux due to charge exchange with the geocorona, $\mathrm{F_{cex}}$. The geocoronal density, equation (1), is based on the results of Wallace *et al.* [1970] using, for convenience, an exponent of 3 rather than 3.07. The range of Wallace *et al.'s* data is about 3-15 $\mathrm{R_E}$. Equation (1) is also very close to the more recent results of Rairden *et al.* [1986] in which a fit to their data over the range 2-11 $\mathrm{R_E}$ with the functional form above gives an 11 $\mathrm{R_E}$ density of 11.3 $\mathrm{cm}^{-3}$ and a power law exponent of 2.92. So, equation (1) seems reasonable given the order-of-magnitude spirit of the calculation.

Following the work of Roelof [1997] and Roelof and Skinner [2000] we write

$$F_{cex} = \int_{r_{mp}}^{\infty} N(R)\,\sigma\, n_{sw} v_{sw}\, dR, \tag{2}$$

where $r_{mp}$ is the distance of the magnetopause from the Earth.

The solar wind neutrals are expected to emerge from the charge exchange collision with their initial velocity, $v_{sw}$, and without the solar wind density, $n_{sw}$, being significantly depleted. Thus, the fraction of the solar wind density we expect to be neutral due to its interaction with the Earth's geocorona is simply

$$\frac{n_{cex}}{n_{sw}} = \int_{r_{mp}}^{\infty} N(R)\,\sigma\, dR, \tag{3}$$

Using equation (1) for the neutral density and taking $\sigma \sim 1.6\text{x}10^{-15}$ cm$^2$ [*Gealy and Van Zyl,* 1987], we get

$$\begin{aligned} \frac{n_{cex}}{n_{sw}} &= 10\,\text{cm}^{-3} \cdot 11^3 \cdot 1.6\text{x}10^{-15}\,\text{cm}^2 \cdot 6371\text{x}10^5\,\text{cm} \cdot \int_{r_{mp}}^{\infty} \frac{dR}{R^3} \\ &= \frac{6.8\text{x}10^{-3}}{r_{mp}^2}, \end{aligned} \tag{4}$$

where $r_{mp}$ is measured in Earth radii.

At standard magnetopause distances of 10 $R_E$, this results in a fraction of about $7\text{x}10^{-5}$, comparable to the expected neutral solar wind component at 1 AU [*Holzer,* 1977; *Gruntman,* 1994; *Gruntman,* 1997] so that this effect under normal circumstances will tend to double the neutral solar wind flux. Of course, 10 $R_E$ is a nominal subsolar magnetopause distance and IMAGE on June 8, 2000 was viewing the flank. However, the magnetopause was also considerably more compressed than normal at this time.

As a final note, we will calculate the ratio of neutral flux to solar wind flux on May 24, 2000 when LENA was observing both the direct neutral solar wind and

the effect of charge exchange with the Earth's geocorona. Referring back to Fig. 3, on this day the LENA sun pulse signal during the enhancement is about 60 counts per spin, which results in 22 counts per second. Unlike the June 8, 2000 event, when the stop microchannel plate was operated at a higher level, the May 24, 2000 event occurred close to the start of science operations when the instrument stop microchannel plate bias level was conservatively lower. Consequently, the 1 keV atomic hydrogen efficiency was $1.5\text{x}10^{-5}$ during this event, and the neutral flux about $1.4\text{x}10^{6}$ $\text{cm}^{-2}\text{s}^{-1}$. The solar wind flux during this enhancement was about $2.8\text{x}10^{9}$ $\text{cm}^{2}\text{s}^{-1}$ which yields a flux ratio of neutrals to solar wind protons of about $5\text{x}10^{-4}$. This supports a direct neutral solar wind to solar wind proton ratio in the low $10^{-4}$s.

## 8. Geophysical Phenomena and Early CME Warning

In the early 1960's, Akasofu [1964a,b] proposed that because neutral hydrogen atoms can penetrate deep into the magnetosphere without being stopped by the geomagnetic field, an incomplete ionization of the solar plasma may be associated with the development of magnetic storms. In particular, it was maintained that neutral hydrogen atoms produced an intense ring current belt and that a flux of $\sim 10^{9}/\text{cm}^{2}/\text{s}$ could effect a main phase at least as intense as -40$\gamma$ (-40 nT).

Brandt and Hunten [1966] criticized Akasofu's work on three grounds: (i) that the neutral fraction at the Earth is 0.1% or less (not the 10% assumed by Akasofu) (ii) that Akasofu's estimate of the current resulting from the neutral flux is too large and (iii) that the neutral flux postulated by Akasofu would produce unobserved optical emissions. Cloutier [1966] also examined Akasofu's arguments and concluded that neutral fluxes of $10^{9}/\text{cm}^{2}/\text{s}$ were highly improbable.

Our results indicate that there is a neutral flux penetrating the magnetosphere that is of the order of $10^{-3} - 10^{-4}$ the solar wind flux, not the $10^{-1}$ required by Akasofu [1964a,b] for his estimates (although Brandt and Hunten [1966] question whether even this level of neutral penetration would be geoeffective). These fluxes include likely contributions from charge exchange in the magnetosheath, which were not considered by Akasofu, although there does not appear to be any reason why these particles would not contribute to Akasofu's mechanism, as well, if it were operative.

Nevertheless, there may be a link between solar wind neutrals and geomagnetic storms. One potential practical application of low energy neutral atom imaging is the advance warning of Earth-directed CMEs. If possible, this could provide geomagnetic storm warnings. Because the triggering of large storms is related to the initial speed of Earthward-directed CMEs, it has been proposed that neutral atoms produced in CMEs in the initial high speed stage can move ahead of the CME as it slows down in its Earthward propagation. These neutrals could be observed at Earth sufficiently early (by a few hours) to provide storm warnings [*Hsieh et al.,* 1992b; *Gruntman,* 1994]. This method is particularly attractive because a LENA-like instrument is considerably less expensive than a solar stereo-type mission which would also allow advance prediction of geomagnetic disturbances [e.g. *Gosling et al.,* 1991].

Although there is no evidence in the five or so hours prior to the CME passage on June 8, 2000 of an enhancement in the neutrals detected by LENA, as mentioned earlier the viewing angle did not contain the Sun direction. However, even if the Sun were in LENA's field-of-view, there would still be the issue of decoupling the contribution due to charge exchange in the magnetosheath from the contribution due

to the CME. This problem would be obviated by placing a LENA-like instrument in interplanetary space and serves as one good argument among many for such a mission.

We mention in passing one other interesting implication of the current work. Bzowski *et al.* [1996] point out that the solar system has in the past and will in the future move through interstellar clouds with densities a factor of $10^3$ higher than the current interstellar density. This is expected to dramatically increase the neutral flux that impinges on the Earth's upper atmosphere. Because monatomic hydrogen is highly reactive, Bzowski *et al.* estimate that if enhanced fluxes were maintained for 10-100 years, they would effect sufficient ozone destruction to create excess solar UV radiation at ground level during past and future epochs when the heliosphere passed through a dense interstellar cloud. Although stopping short of linking interplanetary neutral hydrogen fluxes with dinosaur extinction, this offers an intriguing possibility, especially considering our estimated neutral fluxes appear higher than those assumed by Bzowski *et al.*

## 9. Conclusions

To our knowledge, we have reported the first observations of hydrogen atoms of energy >300 eV consistent with solar wind-type energies from the magnetosheath and interplanetary space streaming throughout the magnetosphere. This work establishes two important facts: (i) the LENA detection technique is now proven viable for the observation of space plasma populations containing hydrogen atoms of solar wind energies and (ii) there is a flux of neutral atoms, about $10^{-3}$-$10^{-4}$ of the solar wind flux, in the magnetosphere. This opens a new window for observation and a new topic for investigation using low energy neutral atoms to remotely sense

space plasmas.

We have reported observations of count rate increases (brightening of features in the two-dimensional images)observed by the LENA imager on May 24, 2000 and June 8, 2000, when a shock driven by a CME associated with a solar flare on June 6, 2000, arrived at the Earth. By establishing that a localized signal which is always present in the LENA data and is observed where the imager field-of-view passes closest to the solar direction is not produced by UV photons or suprathermal particles, we have shown that the enhancements (and likely the pre- and post-event signals) are produced by neutrals originating from the solar wind, possibly in the magnetosheath region outside the magnetosphere. The observed neutral hydrogen energies are greater than 300 eV, consistent with energies characteristic of the solar wind, based on a comparison between LENA time-of-flight spectra from calibration and from this event. In addition, we observed in the solar wind neutral particle signals a composition change associated with the large solar wind velocity jump of the shock passage in the June 8, 2000 event. We estimate, based on LENA efficiencies from calibration data and the observed neutral solar wind flux, a solar wind neutral flux to solar wind ion flux ratio of about $10^{-3}$-$10^{-4}$. This is consistent with predicted neutral solar wind fluxes at 1 AU [*Holzer,* 1977; *Gruntman,* 1994]. However, we point out that a fraction of this signal is due to solar wind charge exchange with the geocorona near the magnetopause. We show simulations of LENA's response to charge exchange in the magnetosheath which corroborates this interpretation. These results show that low energy neutral atom imaging may provide the capability to directly monitor the solar wind and/or magnetosheath from inside the magnetosphere.

**Acknowledgments.** This research is supported by the Explorer Program at NASA's GSFC under Mission Operations and Data Analysis UPN 370-28-20. Michael R. Collier's involvement with the LENA instrument began while he was a National Research Council Resident Research Associate in the Electrodynamics Branch, Code 696. The authors wish to thank Professor Darrel Judge, USC, CA for SOHO/SEM data and Dr. James Green for RPI data. We also wish to acknowledge Evelyn Lee for programming support and Dr. James A. Slavin for helpful Venus conversations and references.

**References**

Akasofu, S.-I., A source of the energy for geomagnetic storms and auroras, *Planet. Space Sci., 12*, 801-833, 1964a.

Akasofu, S.-I., The neutral hydrogen flux in the solar plasma flow - I, *Planet. Space Sci., 12*, 905-913, 1964b.

Barat, M., J.C. Brenot, J.A. Fayeton and Y.J. Picard, Absolute detection efficiency of a microchannel plate detector for neutral atoms, *Rev. Sci. Instrum., 71*, 2050-2052, 2000.

Bauske, R., A.F. Nagy, T.I. Gombosi, D.L. De Zeeuw, K.G. Powell and J.G. Luhmann, A three-dimensional MHD study of solar wind mass loading process at Venus: Effects of photoionization, electron impact ionization, and charge exchange, *J. Geophys. Res., 103*, 23,625-23,638, 1998.

Bertaux, J.L. and J.E. Blamont, Interpretation of Ogo 5 Lyman alpha measurements in the upper geocorona, *J. Geophys. Res., 78*, 80-91, 1973.

Boardsen, S.A., T.E. Eastman, T. Sotirelis and J.L. Green, An empirical model of the high-latitude magnetopause, *J. Geophys. Res., 105*, 23,193-23,219, 2000.

Brandt, J.C. and D.M. Hunten, On ejection of neutral hydrogen from the Sun and the terrestrial consequences, *Planet. Space Sci., 14*, 95-105, 1966.

Bzowski, Maciej, Hans J. Fahr and Daniel Ruciński, Interplanetary neutral particle fluxes influencing the Earth's atmosphere and terrestrial environment, *Icarus, 124*, 209-219, 1996.

Cloutier, Paul A., A comment on "The neutral hydrogen flux in the solar plasma flow" by S.-I. Akasofu, *Planet. Space Sci., 14*, 809-812, 1966.

Collier, Michael R., On generating kappa-like distribution functions using velocity space Lévy flights, *Geophys. Res. Lett., 20*, 1531-1534, 1993.

Collier, Michael R., J.A. Slavin, R.P. Lepping, A. Szabo and K. Ogilvie, Timing accuracy for the simple planar propagation of magnetic field structures in the solar wind, *Geophys. Res. Lett., 25*, 2509-2512, 1998.

Collier, Michael R., D.C. Hamilton, G. Gloeckler, P. Bochsler and R.B. Sheldon, Neon-20, oxygen-16, and helium-4 densities, temperatures, and suprathermal tails in the solar wind determined with WIND/MASS, *Geophys. Res. Lett., 23*, 1191-1194, 1996.

Dessler, A.J., W.B. Hanson and E.N. Parker, Formation of the geomagnetic storm main-phase ring current, *J. Geophys. Res., 66*, 3631-3637, 1961.

Fahr, H.J., Neutral corpuscular energy flux by charge-transfer collisions in the vicinity of the Sun, *Astrophys. and Space Sci., 2*, 496-503, 1968.

Formisano, V., G. Moreno, F. Palmiotto and P.C. Hedgecock, Solar wind interaction with the earth's magnetic field 1. Magnetosheath, *J. Geophys. Res., 78*, 3714-3730, 1973.

Fuselier, S.A., A.G. Ghielmetti, T.E. Moore, M.R. Collier, J.M. Quinn, G.R. Wilson, P. Wurz, S.B. Mende, H.U. Frey, C. Jamar, J.-C. Gerard and J.L. Burch, Ion outflow observed by IMAGE: Implications for source regions and heating mechanisms, *Geophys. Res. Lett.,* submitted, 2001.

Gealy, M.W. and B. Van Zyl, Cross sections for electron capture and loss. I. $H^+$ and $H^-$ impact on H and $H_2$, *Phys Rev. A, 36*, 3091-3099, 1987.

Gosling, J.T., D.J. McComas, J.L. Phillips and S.J. Bame, Geomagnetic activity associated with Earth passage of interplanetary shock disturbances and coronal mass ejections, *J. Geophys. Res., 96*, 7831-7839, 1991.

Groth, Clinton P.T., Darren L. De Zeeuw, Tamas I. Gombosi and Kenneth G. Powell, Global three-dimensional MHD simulation of a space weather event: CME

formation, interplanetary propagation, and interaction with the magnetosphere, *J. Geophys. Res., 105*, 25,053-25,078, 2000.

Gruntman, Michael A., Neutral solar wind properties: Advance warning of major geomagnetic storms, *J. Geophys. Res., 99*, 19,213-19,227, 1994.

Gruntman, Michael, Energetic neutral atom imaging of space plasmas, *Rev. Sci. Instrum., 68*, 3617-3656, 1997.

Grünwaldt, H., M. Neugebauer, M. Hilchenbach, P. Bochsler, D. Hovestadt, A. Bürgi, F.M. Ipavich, K.-U. Reiche, W.I. Axford, H. Balsiger, A.B. Galvin, J. Geiss, F. Gliem, G. Gloeckler, K.C. Hsieh, R. Kallenback, B. Klecker, S. Livi, M.A. Lee, G.G. Managadze, E. Marsch, E. Möbius, M. Scholer, M.I. Verigin, B. Wilken, P. Wurz, Venus tail ray observation near Earth, *Geophys. Res. Lett., 24*, 1163-1166, 1997.

Hodges, R. Richard, Jr. and Brian A. Tinsley, Charge exchange in the Venus ionosphere as the source of the hot exospheric hydrogen, *J. Geophys. Res., 86*, 7649-7656, 1981.

Holzer, Thomas E., Neutral hydrogen in interplanetary space, *Rev. Geophys. and Space Phys., 15*, 467-490, 1977.

Hsieh, K.C., C.C. Curtis, C.Y. Fan and M.A. Gruntman, Techniques for the remote sensing of space plasma in the heliosphere via energetic neutral atoms: A review, Solar Wind Seven (Proceedings of the Third COSPAR Symposium), E. Marsch and R. Schwenn, eds., Pergamon, New York, 357-364, 1992a.

Hsieh, K.C., K.L. Shih, D.J. McComas, S.T. Wu and C.C. Wu, Forecasting the arrival of fast coronal mass ejecta at Earth by the detection of 2-20 keV neutral atoms, Instrumentation for Magnetospheric Imagery, Proceedings SPIE - The International Society for Optical Engineering, S. Chakrabarti (ed.), 1744, 72-78,

1992b.

Hundhausen, A.J., H.E. Gilbert and S.J. Bame, Ionization state of the interplanetary plasma, *J. Geophys. Res., 73*, 5485-5493, 1968.

Judge, D.L., D.R. McMullin, H.S. Ogawa, D. Hovestadt, B. Klecker, M. Hilchenbach, E. Möbius, L.R. Canfield, R.E. Vest, R. Watts, C. Tarrio, M. Kühne and P. Wurz, First solar EUV irradiances obtained from SOHO by the CELIAS/SEM, *Solar Physics, 177*, 161-173, 1998.

Moore, T.E., D.J. Chornay, M.R. Collier, F.A. Herrero, J. Johnson, M.A. Johnson, J.W. Keller, J.F. Laudadio, J.F. Lobell, K.W. Ogilvie, P. Rozmarynowski, S.A. Fuselier, A.G. Ghielmetti, E. Hertzberg, D.C. Hamilton, R. Lundgren, P. Wilson, P. Walpole, T.M. Stephen, B.L. Peko, B. Van Zyl, P. Wurz, J.M. Quinn and G.R. Wilson, The Low-Energy Neutral Atom Imager for IMAGE, *Space Sci. Rev., 91*, 155-195, 2000.

Moore, T.E., M.R. Collier, J.L. Burch, D.J. Chornay, B. El Marji, S.A. Fuselier, A.G. Ghielmetti, B.L. Giles, D.C. Hamilton, F.A. Herrero, J.W. Keller, K.W. Ogilvie, B.L. Peko, J.M. Quinn, T.M. Stephen, G.R. Wilson and P. Wurz, Low energy neutral atoms in the magnetosphere, *Geophys. Res. Lett.,* in press, 2001.

Oberheide, J., P. Wilhelms and M. Zimmer, New results on the absolute ion detection efficiencies of a microchannel plate, *Meas. Sci. Technol., 8*, 351-354, 1997.

Paschalidis, N.P., E.T. Sarris, S.M. Krimigis, R.W. McEntire, M.D. Levine, I.A. Daglis and G.C. Anagnostopoulos, Energetic ion distributions on both sides of the Earth's magnetopause, *J. Geophys. Res., 99*, 8687-8703, 1994.

Paularena, K.I., G.N. Zastenker, A.J. Lazarus, and P.A. Dalin, Solar wind plasma

correlations between IMP 8, INTERBALL-1, and WIND, *J. Geophys. Res., 103*, 14,601-14,617, 1998.

Rairden, R.L., L.A. Frank and J.D. Craven, Geocoronal imaging with Dynamics Explorer, *J. Geophys. Res., 91*, 13,613-13,630, 1986.

Reinisch, B.W., D.M. Haines, K. Bibl, G. Cheney, I.A. Galkin, X. Huang, S.H. Myers, G.S. Sales, R.F. Benson, S.F. Fung, J.L. Green, S. Boardsen, W.W.L. Taylor, J.-L. Bougeret, R. Manning, N. Meyer-Vernet, M. Moncuquet, D.L. Carpenter, D.L. Gallagher and P.H. Reiff, The Radio Plasma Imager Investigation on the IMAGE Spacecraft, *Space Sci. Rev., 91*, 319-359, 2000.

Roelof, E.C., Energetic neutral atom imaging of magnetospheric ions from high and low-altitude spacecraft, *Adv. Space Res., 20*, 341-350, 1997.

Roelof, Edmond C. and Andrew J. Skinner, Extraction of ion distributions from magnetospheric ENA and EUV images, *Space Sci. Rev., 91*, 437-459, 2000.

Schwadron, N.A., J. Geiss, L.A. Fisk, G. Gloeckler, T.H. Zurbuchen and R. von Steiger, Inner source distributions: Theoretical interpretation, implications, and evidence for inner source protons, *J. Geophys. Res., 105*, 7465-7472, 2000.

Stephen, T.M., B. Van Zyl and R.C. Amme, Generation of a fast atomic-oxygen beam from $O^-$ ions by resonant cavity radiation, *Rev. Sci. Instrum., 67*, 1478-1482, 1996.

Vogan, W.S., S.G. Walton, R.L. Champion, The role of O and Cl adsorbates on the secondary emission properties of tungsten, *Surf. Sci., 459*, 14-22, 2000.

Wallace, L., Charles A. Barth, Jeffrey B. Pearce, Kenneth K. Kelly, Donald E. Anderson, Jr. and William G. Fastie, Mariner 5 measurement of the Earth's Lyman alpha emission, *J. Geophys. Res., Space Physics, 75*, 3769-3777, 1970.

Walton, S.G., R.L. Champion and Yicheng Wang, Negative ion emission from a

stainless steel surface due to positive ion collisions, *J. Appl. Phys., 84*, 1706-1707, 1998.

Williams, D.J., E.C. Roelof and D.G. Mitchell, Global magnetospheric imaging, *Rev. of Geophys., 30*, 183-208, 1992.

Wurz, P., M.R. Aellig, P. Bochsler, A.G. Ghielmetti, E.G. Shelley, S.A. Fuselier, F. Herrero, M.F. Smith and T. Stephen, Neutral atom imaging mass spectrograph, *Opt. Eng., 34*, 2365-2376, 1995.

**Figure Captions**

**Figure 1.** A cross section of the LENA instrument showing particle paths through the sensor. Neutral particles (1) enter the instrument through a collimator (2) which filters charged particles. LENA converts neutrals to negative ions through a near specular glancing reflection from a tungsten surface (3). Negative ions from the surface are then collected by the extraction lens (4) which focuses all negative ions with the same energy to a fixed location. In the extraction lens, the ions are accelerated by as much as 20 kV prior to entering the electrostatic deflection system (5). Finally, the ions pass into a time-of-flight/position sensing section (6) where ion mass, energy and angle are determined.

**Figure 2.** An overview of the LENA total event data on May 24, 2000 when the Sun was within LENA's $\pm 45°$ field-of-view. The y-axis shows the LENA spin angle. All valid events are included regardless of the time-of-flight. The bright yellow streak across the plot is the "Sun pulse" which is primarily if not exclusively neutral particles arriving from the direction of the Sun. The white lines around zero degrees represent the angular range of the Earth.

**Figure 3.** Plot showing the LENA sun sector hydrogen count rate (i.e. events falling in the hydrogen time-of-flight range) during the May 24, 2000 event. Also plotted is the solar wind proton flux observed by the WIND spacecraft. Note the strong correlation during the peak of the event around 0200 UT. At this time, RPI data place IMAGE inside the magnetopause. Because LENA's field-of-view includes the direction of the Sun during this time period, the sun pulse comprises both solar wind neutrals that have charge exchanged in the interplanetary medium as well as solar wind neutrals that have charge exchanged in the magnetosheath with the

Earth's geocorona.

**Figure 4.** Cartoon showing LENA viewing geometry during the June 8, 2000 event. LENA observes two possible sources of solar wind neutral atoms. First, LENA observes the direct neutral solar wind formed from charge exchange with interstellar neutrals and dust grains when it falls within its field-of-view. Second, LENA observes solar wind ions charge exchanging in the near-Earth magnetosheath. It is argued that the June 8, 2000, data may be primarily the latter whereas during the May 24, 2000 event LENA likely observes both components.

**Figure 5.** A LENA spectrogram showing the combined hydrogen and oxygen count rate as a function of time on June 8, 2000. The y-axis shows the spacecraft spin angle. The direction and angular range of the Earth are indicated by the white dashed lines. The "sun pulse" is the streak hovering around 180°. This signal increases by about a factor of two when the shock passes at 0911 UT.

**Figure 6.** EUV data showing photon flux from SOHO/CELIAS/SEM on June 6-8, 2000. The upper solid line is the photon flux from 0.1-50 nm and the lower dashed curve shows the photon flux from 24-34 nm. The flares on June 6 and 7 are apparent in the data. However, there is no EUV enhancement during the event on June 8, showing that LENA is not responding to UV light at this time.

**Figure 7.** A comparison of the LENA sun sector event count rate and the ACE/EPAM flux of ions between 47 and 65 keV on June 8, 2000. The energetic particle flux shows a step-function increase whereas the LENA count rate rises and falls over the course of about an hour. This suggests that LENA is not responding to energetic particles during this time period.

**Figure 8.** A comparison between the LENA sun sector event count rate data and the solar wind ram pressure on June 8, 2000. This figure also shows with black bars along the upper x-axis when the IMAGE spacecraft based on the high-latitude magnetopause model of Boardsen *et al.* [2000] is inside the magnetosphere. The model predicts that during the June 8, 2000 event IMAGE moved back and forth across the magnetopause many times. This implies that if IMAGE were responding to energetic particles during this time, there would be changes in the signal corresponding to the boundary crossings. Because no such changes are observed and the distribution is less isotropic than would be expected from energetic particles, it is concluded that LENA is not responding to suprathermal ions during this time period. Both the solar wind ram pressure and the Boardsen *et al.* model results are derived from WIND spacecraft data.

**Figure 9.** The two panels in this figure show a comparison of the time-of-flight spectra from the Denver University calibration resulting from incident atomic hydrogen. The top panel shows a time-of-flight spectrum resulting from 30 eV atomic hydrogen. Note the absence of a sputtered oxygen peak. The lower panel shows a time-of-flight spectrum resulting from 1 keV atomic hydrogen. At this higher, solar wind energy, a sputtered oxygen peak is apparent in the time-of-flight data.

**Figure 10.** This figure shows a LENA time-of-flight spectrum taken during the June 8, 2000 event from 0900-1100 UT. The spectrum only includes events coming from the general direction of the Sun. The pronounced oxygen peak in the spectrum indicates that the neutral hydrogen energies are >300 eV, consistent with expected neutral solar wind energies.

**Figure 11.** The jump in solar wind speed observed by WIND during the shock pas-

sage on June 8, 2000, indicated by the solid line and left hand y-axis, is reflected in the ratio of atomic hydrogen to sputtered oxygen signal observed by LENA coming from the direction of the Sun, indicated by the solid circles and right hand y-axis. The data in this figure are integrated counts from the Sun direction over all spins during the one hour intervals. The hydrogen peak was taken to be channels 151-190 and the oxygen peak was taken to be channels 401-1000. A background rate was subtracted off both the hydrogen and oxygen peaks based on the number of counts appearing between channels 301-400, where no peak is expected. The count rates during this period are low enough so that the microchannel plates are not saturating. Because IMAGE is inside the magnetosphere during most of the time period covered by Fig. 11, these results indicate that low energy neutral atom imagers can directly monitor interplanetary conditions from inside the magnetosphere.

**Figure 12.** This figure shows a simulation of LENA's response to 4 keV hydrogen atoms on June 8, 2000 (day 160) resulting from solar wind charge exchange with the Earth's geocorona in the magnetosheath. The simulation uses the MHD model BatsRus of T. Gombosi at the University of Michigan, integrating from 8 $R_E$ on out. The dashed line shows the spin angle at which LENA looks closest to the Sun, although the Sun is outside of LENA's $\pm 45°$ field-of-view at this time. Nevertheless, LENA sees a clear "Sun pulse" which is really charge exchange in the magnetosheath. The geocoronal neutral density is assumed spherically symmetric. The solid lines represent the angular extent of the Earth. The signal is dimmer in the second half of the day relative to the first because of the effect of dipole tilt in the model. 4 keV is about the energy of solar wind protons after the shock on June 8, 2000.

LENA Instrument Characteristics

| parameter | character | notes |
|---|---|---|
| field-of-view | 90° azimuthal<br>360° polar | $2\pi$ steradian total<br>(1/2 the sky) |
| H energy sensitivity | 15-20 eV cut-off<br>response to >1 keV | |
| H calibrated energies | 20, 30, 100, 200,<br>300, 1000 eV | |
| pixel size | 8°x8° | 0.02 steradians |
| accumulation interval | 2.7 seconds | 1/45 of 2 minute<br>IMAGE spin period |

**Table 1**

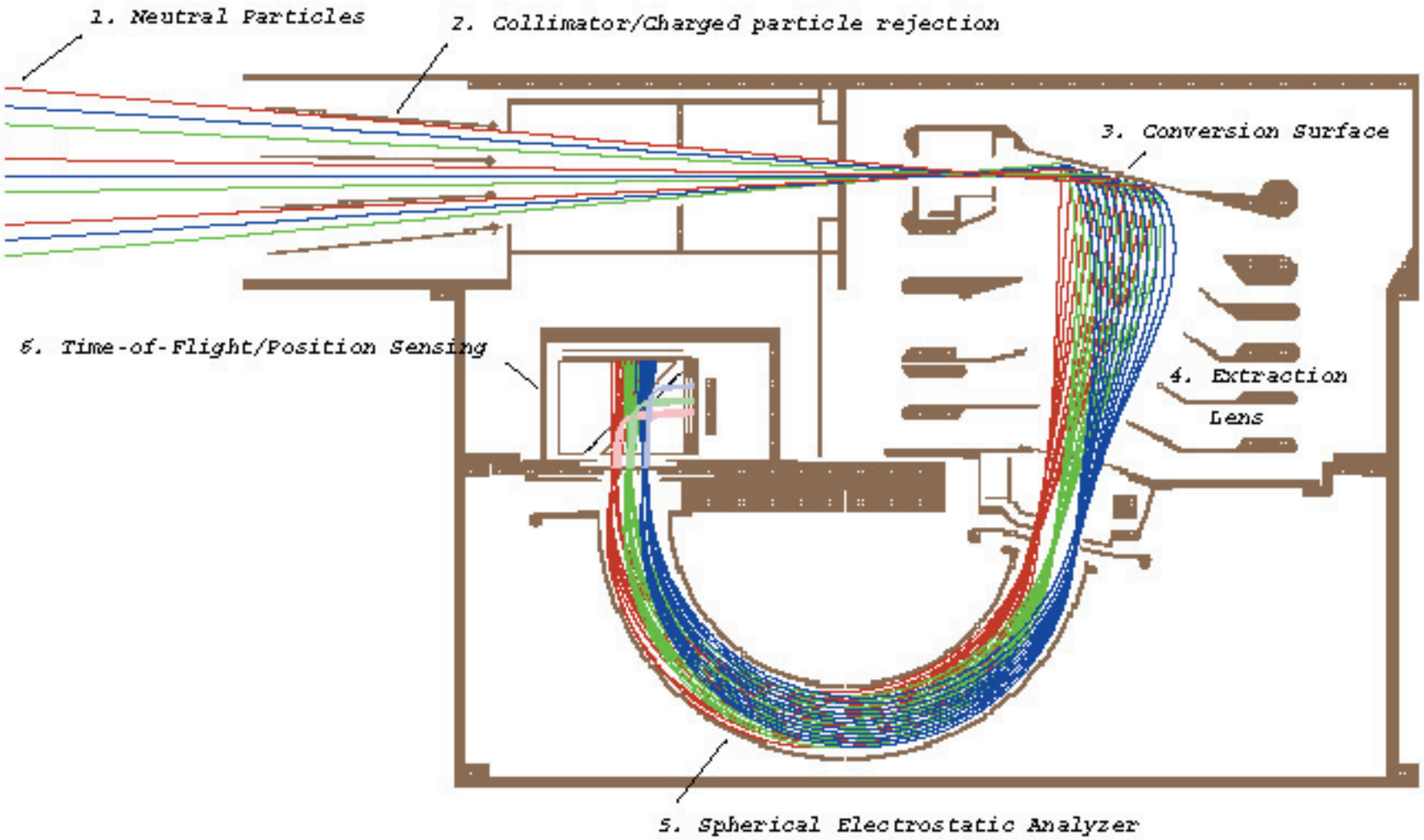
1. Neutral Particles
2. Collimator/Charged particle rejection
3. Conversion Surface
4. Extraction Lens
5. Spherical Electrostatic Analyzer
6. Time-of-Flight/Position Sensing

figure 1

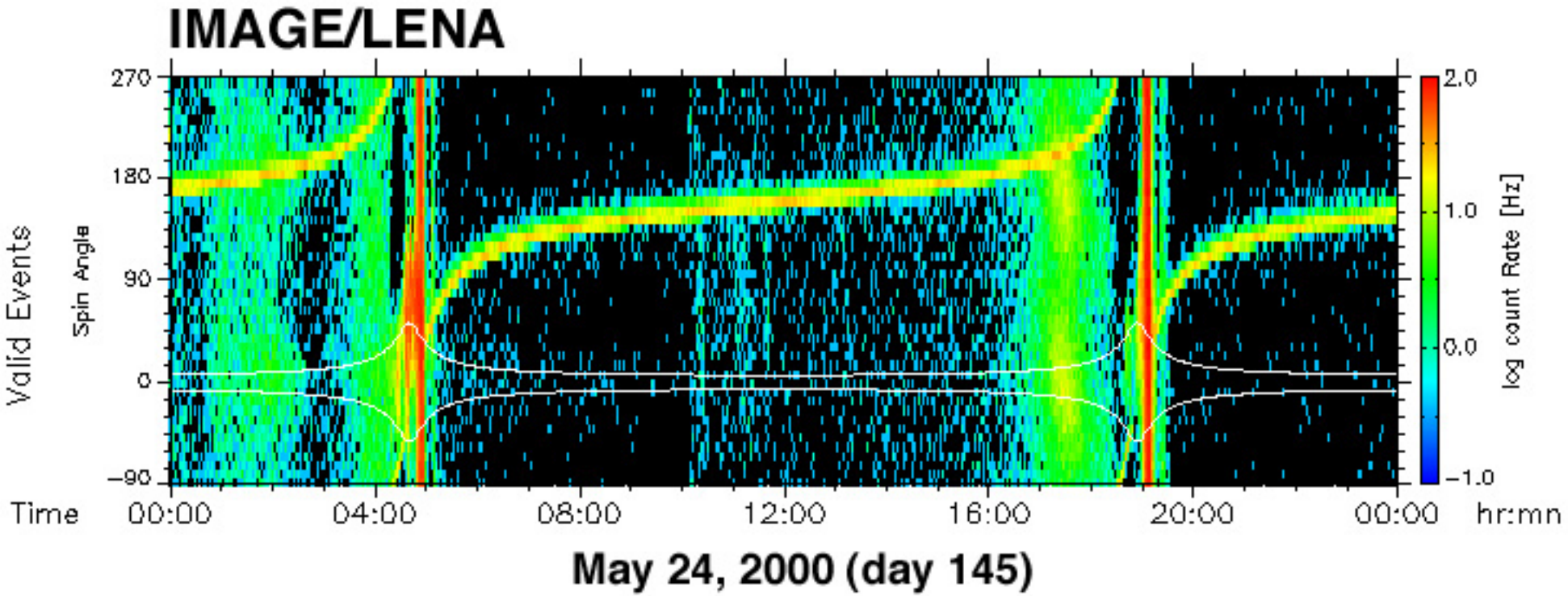
IMAGE/LENA
Valid Events
Spin Angle
270
180
90
0
−90
Time
00:00
04:00
08:00
12:00
16:00
20:00
00:00
hr:mn
2.0
1.0
0.0
−1.0
log count Rate [Hz]
May 24, 2000 (day 145)

figure 2

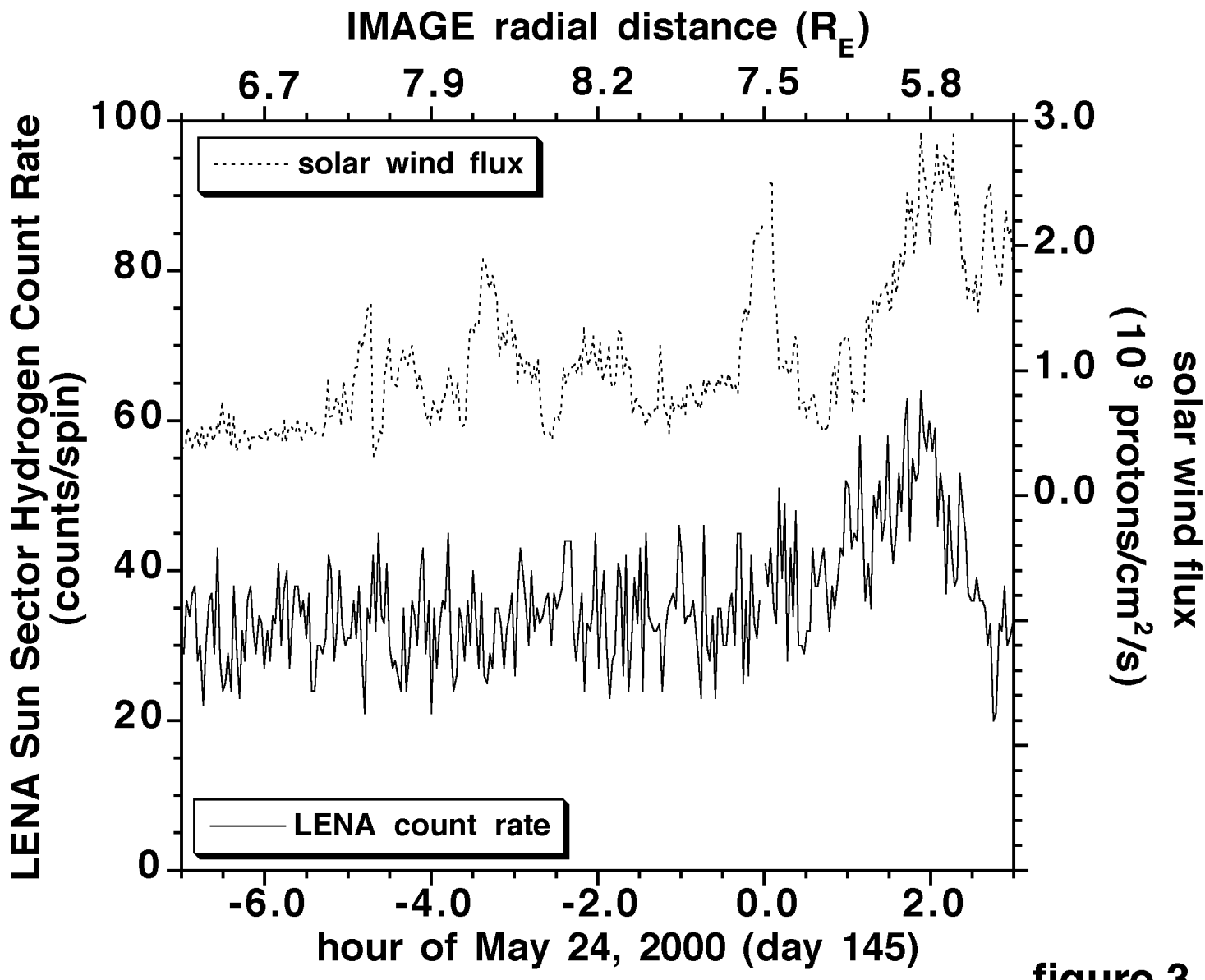
IMAGE radial distance ($R_E$)
6.7
7.9
8.2
7.5
5.8
solar wind flux
LENA count rate
LENA Sun Sector Hydrogen Count Rate (counts/spin)
solar wind flux ($10^9$ protons/cm$^2$/s)
100
80
60
40
20
0
3.0
2.0
1.0
0.0
-6.0
-4.0
-2.0
0.0
2.0
hour of May 24, 2000 (day 145)

figure 3

# Two Sources of Solar Wind Neutral Atoms

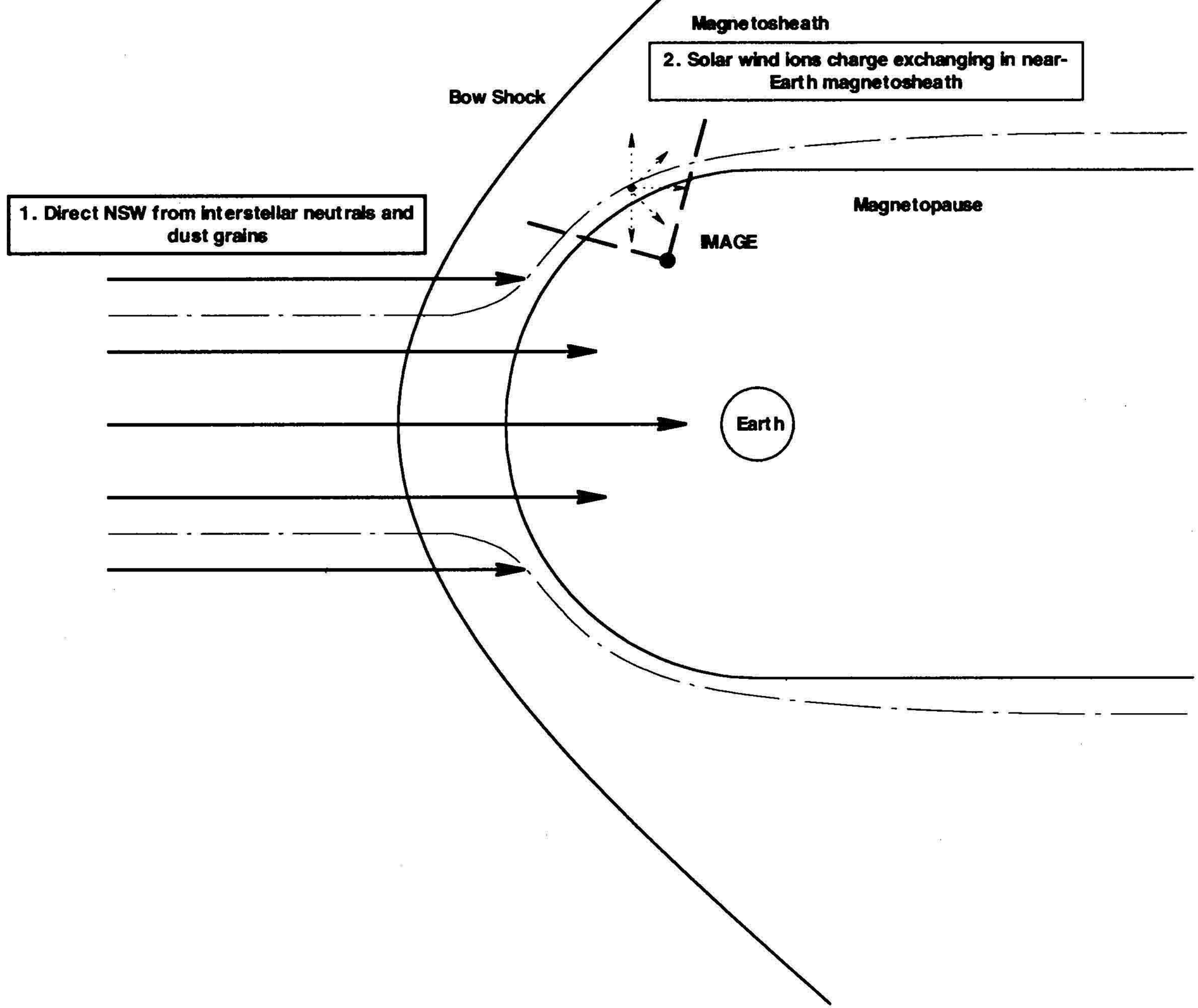


figure 4

# IMAGE/LENA

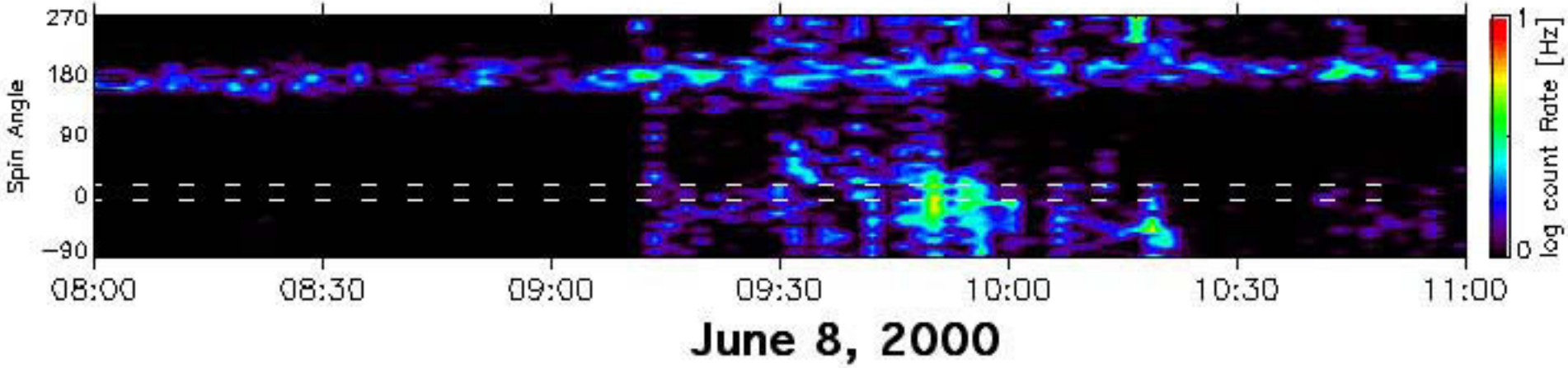


figure 5

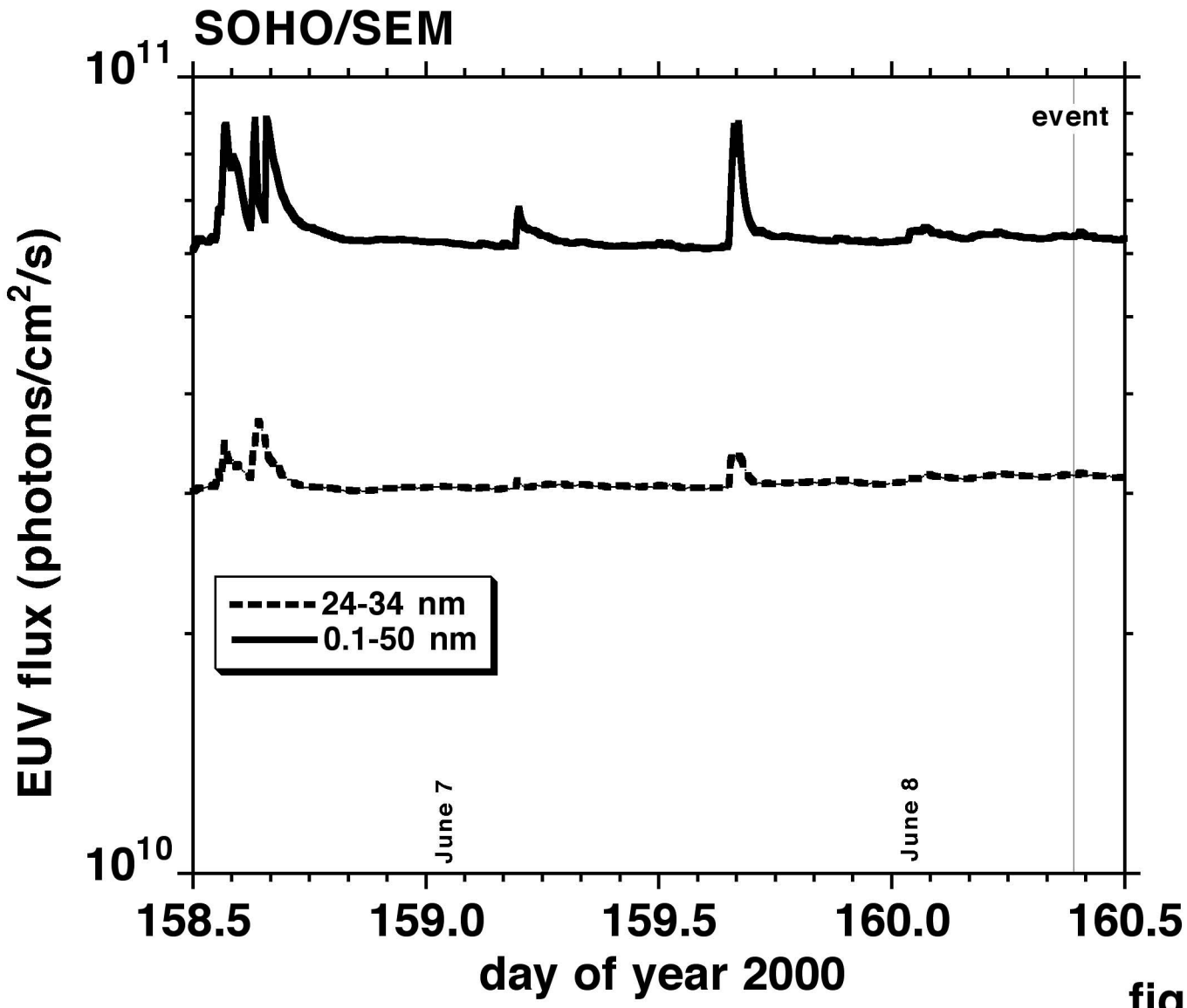
SOHO/SEM
$10^{11}$
$10^{10}$
event
24-34 nm
0.1-50 nm
June 7
June 8
EUV flux (photons/cm$^2$/s)
158.5
159.0
159.5
160.0
160.5
day of year 2000

figure 6

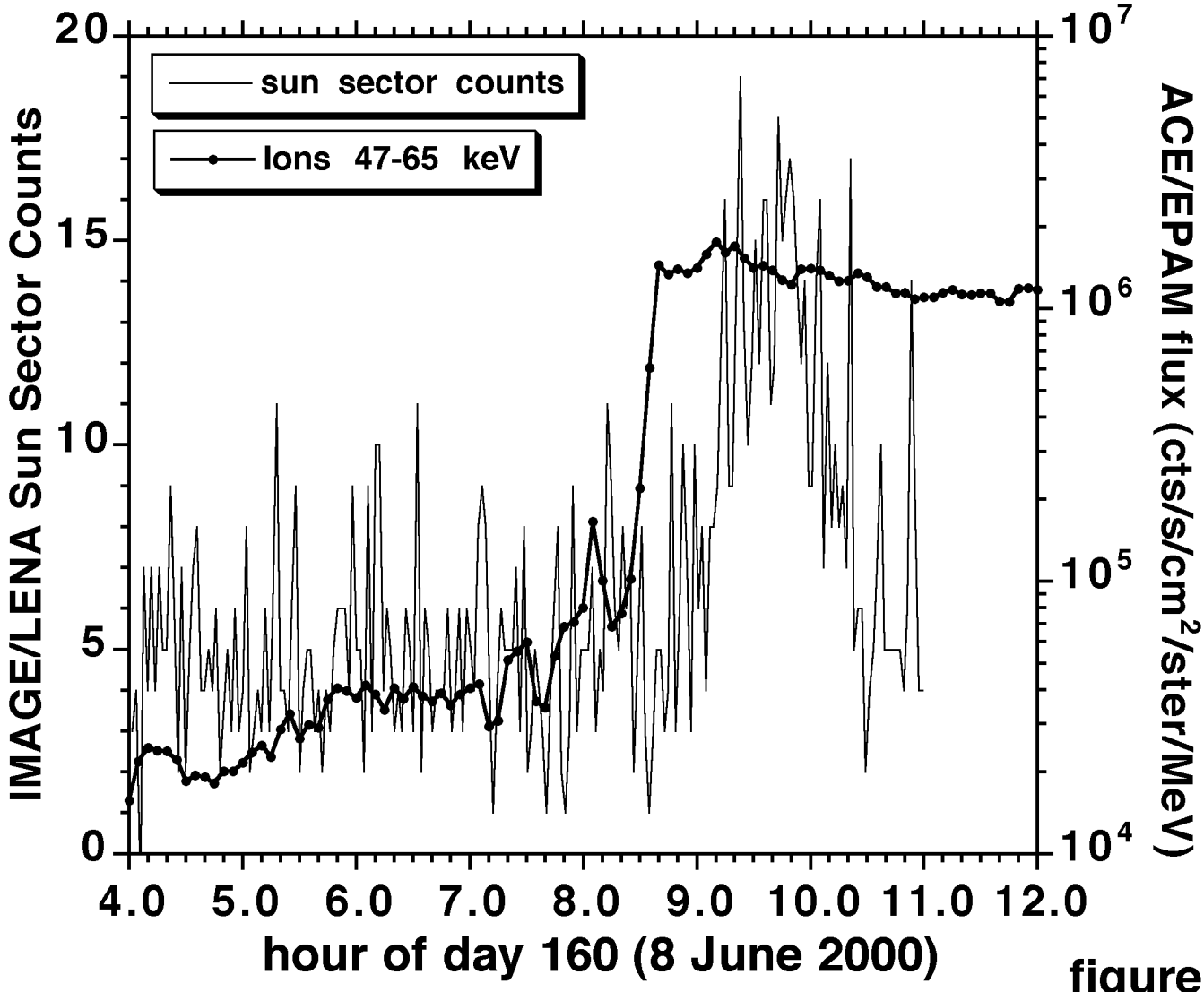
sun sector counts
Ions 47-65 keV
IMAGE/LENA Sun Sector Counts
ACE/EPAM flux (cts/s/cm²/ster/MeV)
hour of day 160 (8 June 2000)
0
5
10
15
20
4.0
5.0
6.0
7.0
8.0
9.0
10.0
11.0
12.0
10⁴
10⁵
10⁶
10⁷

figure 7

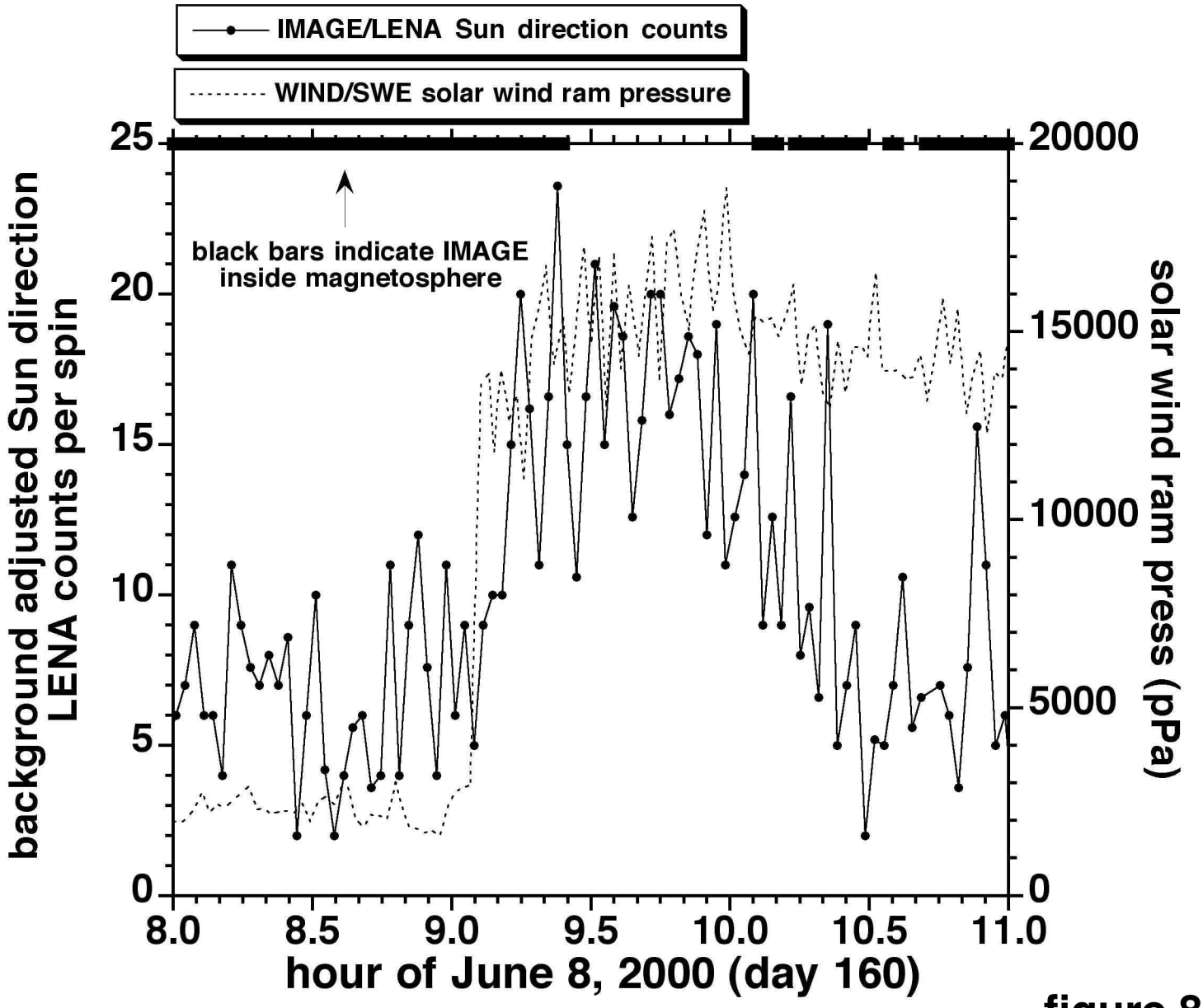
IMAGE/LENA Sun direction counts
WIND/SWE solar wind ram pressure
black bars indicate IMAGE inside magnetosphere
background adjusted Sun direction LENA counts per spin
solar wind ram press (pPa)
hour of June 8, 2000 (day 160)
0
5
10
15
20
25
0
5000
10000
15000
20000
8.0
8.5
9.0
9.5
10.0
10.5
11.0

figure 8

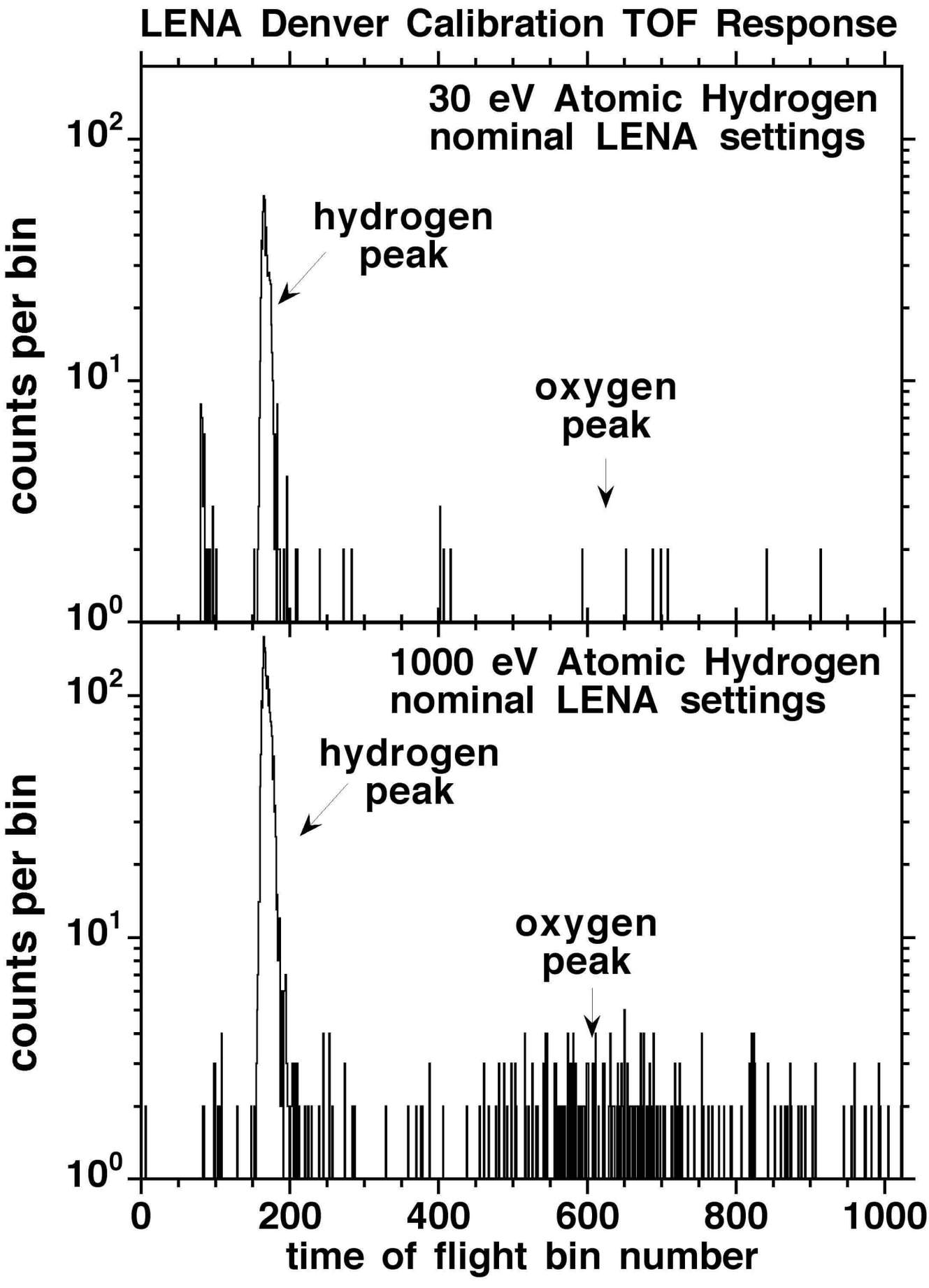
LENA Denver Calibration TOF Response
30 eV Atomic Hydrogen
nominal LENA settings
hydrogen
peak
oxygen
peak
counts per bin
1000 eV Atomic Hydrogen
nominal LENA settings
hydrogen
peak
oxygen
peak
counts per bin
0
200
400
600
800
1000
time of flight bin number

figure 9

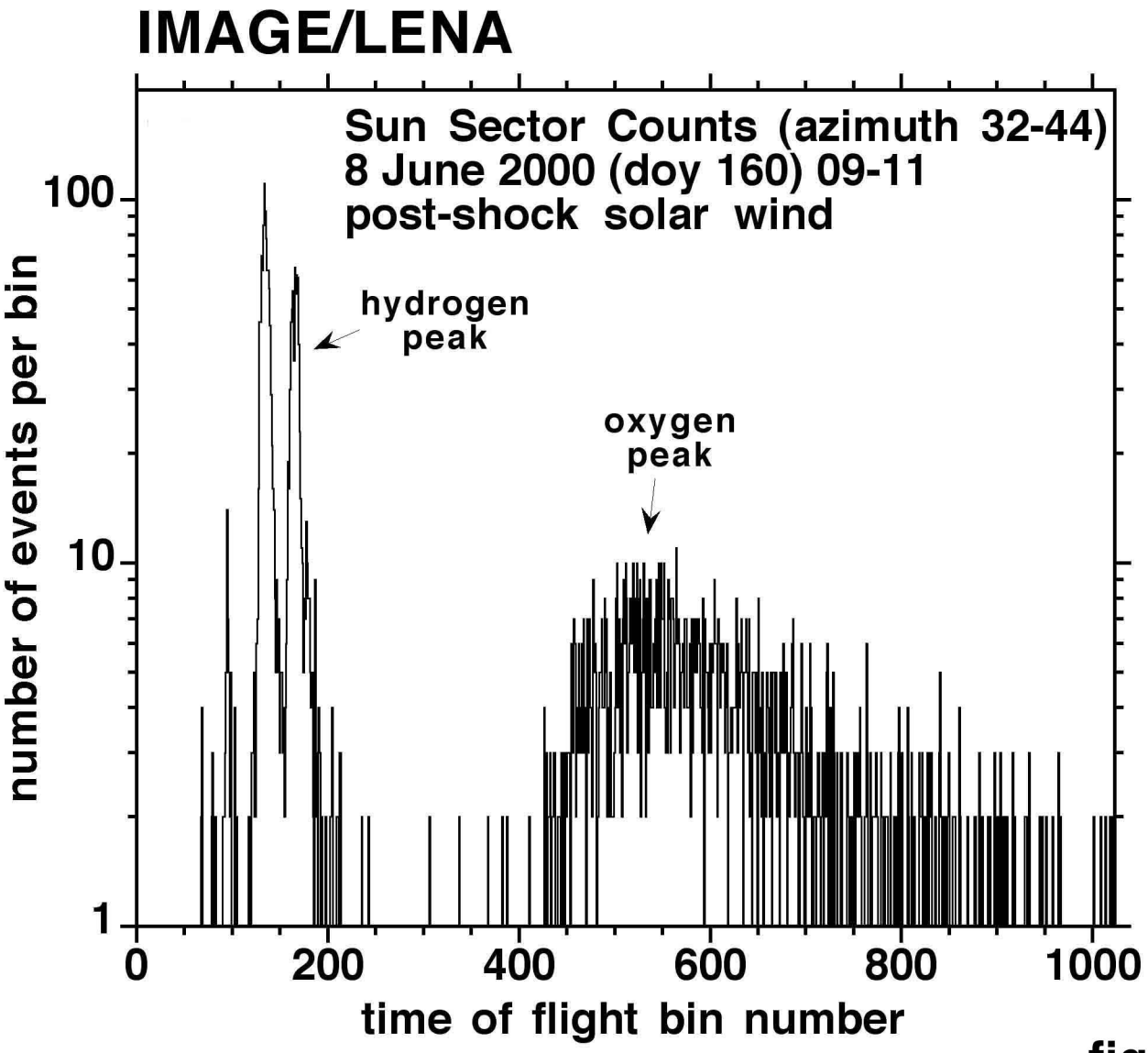
IMAGE/LENA
Sun Sector Counts (azimuth 32-44)
8 June 2000 (doy 160) 09-11
post-shock solar wind
hydrogen peak
oxygen peak
number of events per bin
100
10
1
0
200
400
600
800
1000
time of flight bin number

figure 10

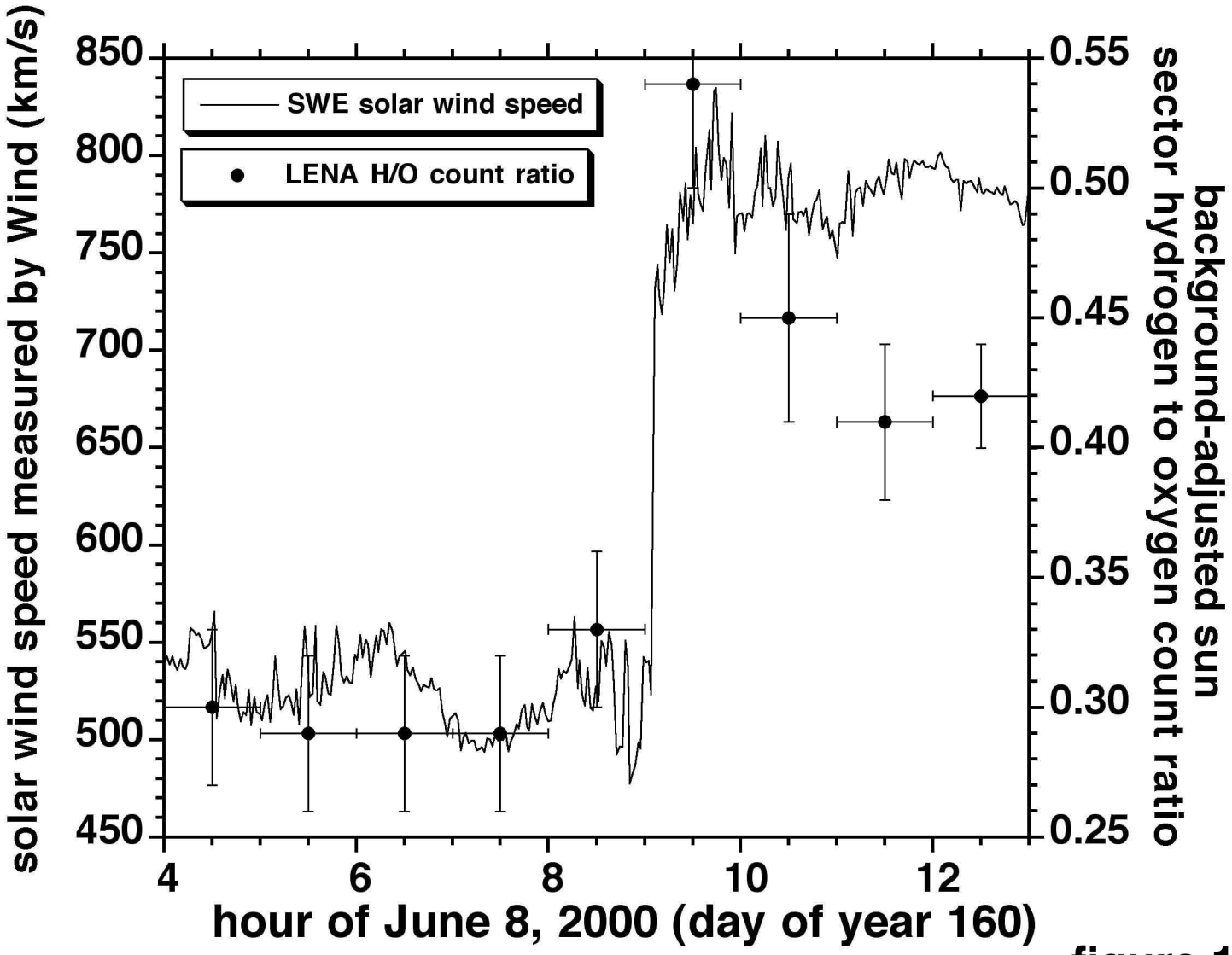
SWE solar wind speed
LENA H/O count ratio
solar wind speed measured by Wind (km/s)
background-adjusted sun sector hydrogen to oxygen count ratio
hour of June 8, 2000 (day of year 160)
850
800
750
700
650
600
550
500
450
0.55
0.50
0.45
0.40
0.35
0.30
0.25
4
6
8
10
12

figure 11

# LENA RESPONSE TO SOLAR WIND CHARGE EXCHANGE WITH THE EARTH's GEOCORONA

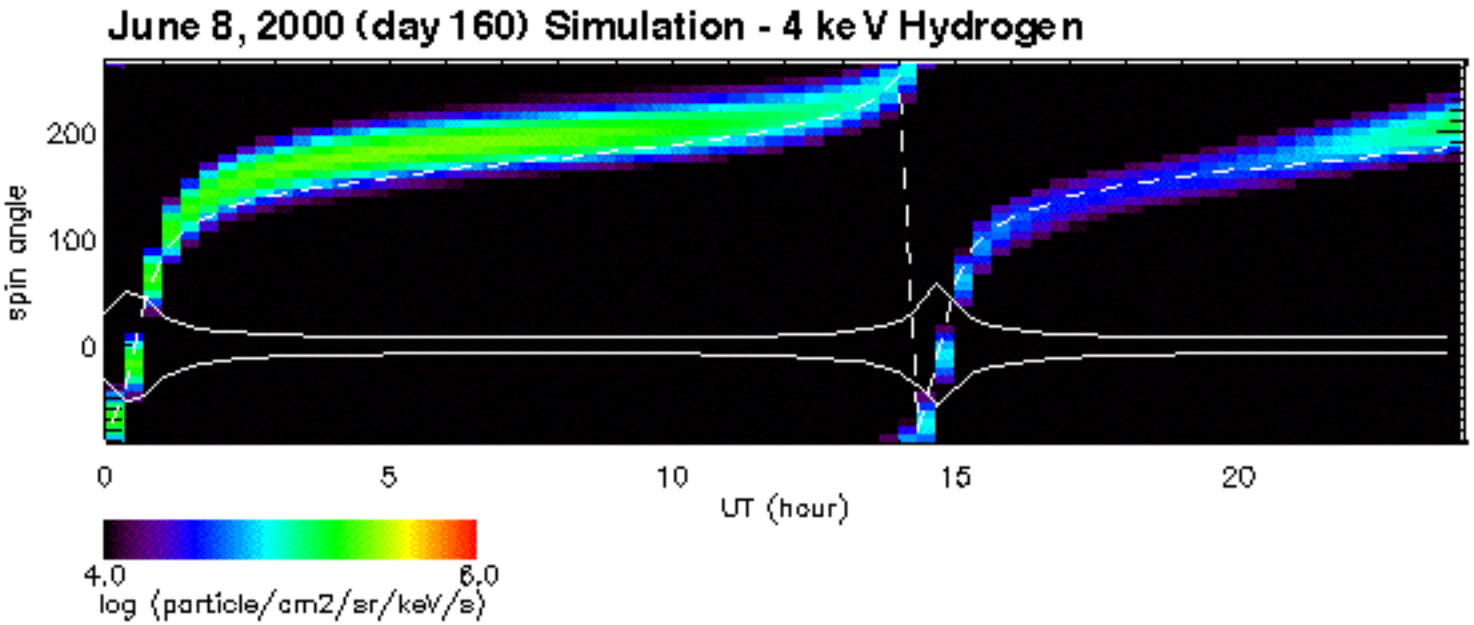


figure 12